Journal of Alloys and Compounds 489 (2010) 140–145

Contents lists available at ScienceDirect

Journal of Alloys and Compounds

journal homepage: www.elsevier.com/locate/jallcom

Elasticity and thermodynamic properties of α-Ta_4AlC_3 under pressure

Feng Peng[a,*], Dong Chen[b], Xiangdong Yang[c]

[a] *College of Physics and Electronic Information, Luoyang Normal University, Luoyang 471022, China*
[b] *School of Physics and Electronic Engineering, Xinyang Normal University, Xinyang 464000, China*
[c] *Institute of Atomic and Molecular Physics, Sichuan University, Chengdu 610065, China*

ARTICLE INFO

Article history:
Received 4 May 2009
Received in revised form 8 September 2009
Accepted 9 September 2009
Available online 16 September 2009

PACS:
62.20.−x
62.50.−p
65.40.−b
71.15.Mb

Keywords:
Ta_4AlC_3
Density functional theory
Elasticity
High pressure

ABSTRACT

First-principles calculations of the crystal structure and the elastic properties of α-Ta_4AlC_3 have been carried out with the plane-wave pseudopotential density functional theory method. The calculated values are in very good agreement with experimental data as well as with some of the existing model calculations. The pressure dependence of the elastic constants c_{ij}, the aggregate elastic moduli (B, G, E), the Poisson's ratio, and the elastic anisotropy has been investigated. Using the quasi-harmonic Debye model considering the phonon effects, the temperature and pressure dependencies of isothermal bulk modulus, and the thermal expansions, and Grüneisen parameters, as well as Debye temperatures are investigated systematically in the ranges of 0–60 GPa and 0–1500 K as well as compared to available data.

1. Introduction

The $M_{n+1}AX_n$ (MAX) compounds, have attracted great attention these last few years due to these compounds exhibit unique properties [1–5], such as low density, high elastic moduli, good high-temperature stability, high thermal and electrical conductivities, excellent thermal shock resistance, damage tolerance and micro-scale ductility at room temperature. Ta_4AlC_3, a new member of the family of multifunctional nanolaminated ceramics known as the MAX phases has drawn a lot of attention recently [6–14]. Ta_4AlC_3 has recently been synthesized either in the form of polycrystals [6–10] or single crystals [11]. The bulk modulus of Ta_4AlC_3 has been determined by Palmquist et al. to be 261 GPa, which is so far the highest for any MAX phase [6]. Ta_4AlC_3 was found to crystallize in a hexagonal structure with the space group $P63/mmc$ (no. 194) [6–11]. Lin et al. [8,9] presented high-resolution transmission electron microscopy (HRTEM) images showing that their hot-pressed Ta_4AlC_3 samples exhibited a different stacking sequence from the structure of Ti_4AlN_3. A Rietveld refinement confirmed their structure and explained the large differences between experimental and calculated data observed by Manoun et al. [7]. Then, Eklund et al. [10] showed that Ta_4AlC_3 exhibited the original Ti_4AlN_3 structure. Recently, Wang et al. [12] and Du et al. [13] and Deng et al. [15,16] studied the polymorphism of Ta_4AlC_3 from first-principles calculations.

The study of material properties under high pressure and temperature is important in a variety of situations in physics, astrophysics and related sciences. Among these properties, the elastic constants, phonon frequencies and equations of state (EOS) are fundamental for solids. An accurate description of the elastic properties for solids are extremely important, because these play significant roles in determining some materials properties, such as interatomic forces, phase transition, transport coefficients, and electron–phonon interactions. Elastic properties are also linked thermodynamically with specific heat, thermal expansion, Debye temperature, and Grüneisen parameter. In particular, they provide information on the stability and stiffness and lattice dynamical considerations of materials [17].

Therefore, in this work we predict the structural stability, and the systematics of elastic and thermodynamic properties of α-Ta_4AlC_3 under high pressure. We find that α-Ta_4AlC_3 has low density, high elastic moduli, high-temperature stability, high thermal and micro-scale ductility at room temperature. This paper is organized as follows: the computational methods are described firstly. Elastic and thermodynamic properties of α-Ta_4AlC_3 under

---

* Corresponding author.
E-mail address: pengfengscu@gmail.com (F. Peng).

0925-8388/$ – see front matter © 2009 Elsevier B.V. All rights reserved.
doi:10.1016/j.jallcom.2009.09.035

Table 1
The lattice constants (Å), bulk and shear moduli (GPa), Poisson ratio, and the elastic constants (GPa) for α-Ta_4AlC_3.

	a	c	c/a	B	G	E	ν	c_{11}	c_{12}	c_{13}	c_{33}	c_{44}
Present	3.189	24.552	7.699	260	141	359	0.269	493	161	155	418	192
Exp. [11]	3.113	24.112										
Ref. [13]	3.1344	24.2675	7.7423	266.3			0.27					
Exp. [10]	3.10884	24.0776	7.7449									
Exp. [5]					132	324						
Ref. [12]								496	154	181	417	200
Ref. [14]-GGA								495	164	157	421	196
Ref. [14]-LDA								437	158	197	416	165
Ref. [15]	3.138	24.163	7.70	247				454	157	156	376	201

high pressure are presented in detail later. Finally, a brief summary and conclusions are given.

2. Computational details and theory

2.1. Computational details

In this work, all calculations were performed using the plane-wave pseudopotential density functional theory (DFT) [18]. Vanderbilt-type non-local ultrasoft pseudopotentials (USPP) [19] are employed to describe the electron–ion interactions. The effects of exchange–correlation interaction are treated within the generalized gradient approximation (GGA) of Wu–Cohen (WC) [20]. In the structure calculation, a plane wave basis set with energy cut-off 650.00 eV is used. Pseudo-atomic calculations are performed for C $2s^22p^2$ and Al $3s^23p^1$ and Ta $5d^36s^2$. For the Brillouin-zone sampling, the 11 × 11 × 3 Monkhorst–Pack mesh is adopted. The self-consistent convergence of the total energy is 10^{-6} eV/atom and the maximum force on the atom is 10^{-4} eV/Å. All the total energy electronic structure calculations are implemented by the CASTEP code [21].

2.2. Structural properties

The energy–volume (E–V) curve can be obtained by fitting the calculated E–V data to the Birch–Murnaghan EOS [22]

$$\Delta E(V) = E - E_0 = B_0V_0\left[\frac{V_n}{B'_0} + \frac{1}{1-B'_0} + \frac{V_n^{1-B'_0}}{B'_0(B'_0-1)}\right]. \tag{1}$$

where E_0 is the equilibrium energy. The pressure P versus the normalized volume V_n is obtained through the following relationship

$$P = -\frac{\mathrm{d}E}{\mathrm{d}V} = \frac{B_0}{B'_0}[V_n^{-B'_0} - 1]. \tag{2}$$

where $B'_0 = \mathrm{d}B_0/\mathrm{d}P$ and B_0 are the pressure derivative of the bulk modulus and zero pressure bulk modulus, respectively.

To calculate the total energy E and the corresponding volume V, a series of different lattice parameters a and c are taken to obtain the total energy over a wide volume range of 0.8–1.2V_0, where V_0 is the zero pressure equilibrium primitive cell volume. The equilibrium lattice parameters a and c (Table 1) can be obtained by two-dimensional scanning the total energy. The calculated equilibrium lattice parameters and bulk modulus B are in good agreement with experimental data [10,11] and other theoretical results [13,15,16], respectively. The ratios a/a_0, c/c_0, and V/V_0 (where a_0, c_0 are the zero pressure and temperature equilibrium lattice constants) as functions of the applied pressure together with the experimental result are plotted in Fig. 1. Our obtained data are consistent well with the experiment [7].

2.3. Elasticity

To calculate the elastic constants under hydrostatic pressures, the non-volume conserving strains are adopted because this method is consistent with our calculated elastic constants using the stress–strain coefficients, which are appropriate for the calculation of the elastic wave velocities. The elastic constants c_{ijkl}, with respect to the finite strain variables, are defined as [23–25]

$$c_{ijkl} = \left(\frac{\partial\sigma_{ij}(x)}{\partial e_{kl}}\right)_X. \tag{3}$$

where σ_{ij} and e_{kl} are the applied stress and Eulerian strain tensors, and X and x are the coordinates before and after the deformation. For the isotropic stress, we have [24–26]

$$c_{ijkl} = C_{ijkl} + \frac{P}{2}(2\delta_{ij}\delta_{kl} - \delta_{il}\delta_{jk} - \delta_{ik}\delta_{jl}),$$

$$C_{ijkl} = \left(\frac{1}{V(x)}\frac{\partial^2 E(x)}{\partial e_{ij}\partial e_{kl}}\right)_X. \tag{4}$$

where C_{ijkl} denotes the second-order derivatives with respect to the infinitesimal strain (Eulerian), and δ is the finite strain variable. For the α-Ta_4AlC_3, there are five independent elastic constants, i.e. c_{11},

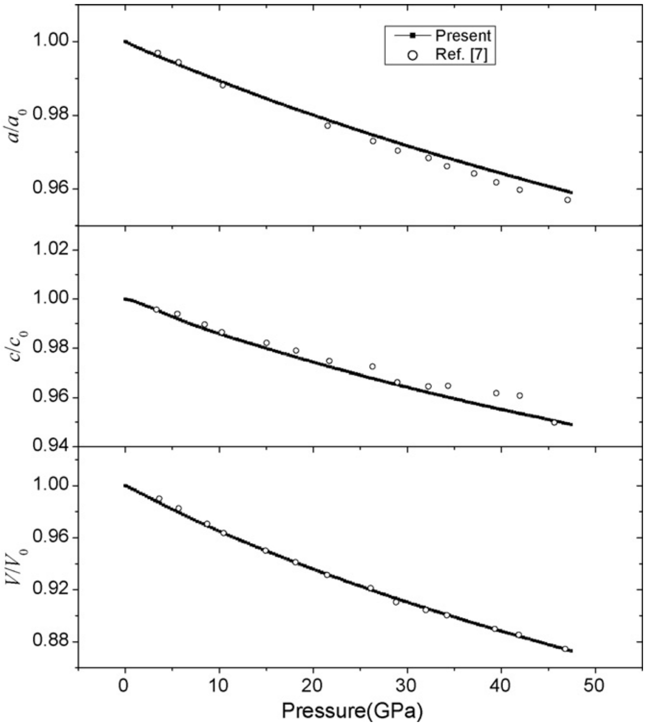

Fig. 1. The variations about the ratios of c/c_0, a/a_0, V/V_0 with the applied pressure for α-Ta_4AlC_3.

c_{12}, c_{13}, c_{33}, and c_{44}. In our calculations, for all strains, $\delta = \pm 0.0018$, ± 0.003, ± 0.0006 are taken to calculate the total energies E for the strained crystal structure, respectively.

Our calculated elastic constants c_{ij} of the α-Ta_4AlC_3 at zero pressure and zero temperature are listed in Table 1. Our obtained data are consistent well with other calculations [12,14,15]. From the independent elastic constants above, the theoretical polycrystalline elastic modulus can be obtained. There are two approximation methods to calculate the polycrystalline modulus, namely the Voigt method [27] and the Reuss method [28]. The Voigt (G_V) and Reuss (G_R) bulk moduli are given by

$$B_V = \frac{1}{9}(2(c_{11} + c_{12}) + c_{33} + 4c_{13}). \tag{5}$$

$$B_R = \frac{(c_{11} + c_{12})c_{33} - 2c_{13}^2}{c_{11} + c_{12} + 2c_{33} - 4c_{13}}. \tag{6}$$

The shear moduli can be estimated by

$$G_V = \frac{1}{30}(c_{11} + c_{12} + 2c_{33} - 4c_{13} + 12c_{44} + 12c_{66}). \tag{7}$$

$$G_R = \frac{5}{4}\frac{((c_{11} + c_{12})c_{33} - 2c_{13}^2)^2 c_{44}c_{66}}{3B_V c_{44}c_{66} + ((c_{11} + c_{12})c_{33} - 2c_{13}^2)^2 (c_{44} + c_{66})}. \tag{8}$$

where $c_{66} = (1/2)(c_{11} - c_{12})$. The arithmetic average of the Voigt and the Reuss bounds is called the Voigt–Reuss–Hill (VRH) average, which is often used to calculate elastic moduli of polycrystals. The VRH averages for shear modulus (G) and bulk modulus (B) are given by

$$G = \frac{1}{2}(G_R + G_V). \tag{9}$$

$$B = \frac{1}{2}(B_R + B_V). \tag{10}$$

The polycrystalline Young's modulus (E), and the Poisson's ratio (ν) are then calculated by

$$E = \frac{9BG}{3B + G}. \tag{11}$$

$$\nu = \frac{3B - 2G}{2(3B + G)}. \tag{12}$$

The elastic Debye temperature (Θ_D) can be estimated from the average sound velocity v_m, by the following equation [29]

$$\Theta_D = \frac{h}{k}\left[\frac{3n}{4\pi}\left(\frac{N_A \rho}{M}\right)\right]^{1/3} v_m. \tag{13}$$

where h is the Planck's constants, k the Boltzmann's constant, N_A the Avogadro's number, n the number of atoms in the molecule, M the molecular weight, and ρ is the density. The average wave velocity v_m is approximately calculated from

$$v_m = \left[\frac{1}{3}\left(\frac{2}{v_s^3} + \frac{1}{v_p^3}\right)\right]^{-1/3}. \tag{14}$$

where v_p and v_s are the compressional and shear wave velocities, respectively, which can be obtained from Navier's equation [30]

$$v_p = \sqrt{\left(B + \frac{4}{3}G\right)\frac{1}{\rho}}. \tag{15}$$

$$v_s = \sqrt{\frac{G}{\rho}}. \tag{16}$$

2.4. Thermodynamic properties

In order to obtain the thermodynamic properties of α-Ta_4AlC_3, the quasi-harmonic Debye model [31] is introduced, in which the phonon effects are considered and the non-equilibrium Gibbs function $G^*(V; P, T)$ takes the form of

$$G^*(V; P, T) = E(V) + PV + A_{Vib}(\Theta(V); T) \tag{17}$$

Here $E(V)$ is the total energy per unit cell for α-Ta_4AlC_3, $\Theta(V)$ is the Debye temperature, and the vibrational Helmholtz free energy A_{Vib} can be written by [32,33]

$$A_{Vib}(\Theta; T) = nKT\left[\frac{9}{8}\frac{\Theta}{T} + 3\ \ln(1 - e^{-\Theta/T}) - D\left(\frac{\Theta}{T}\right)\right]. \tag{18}$$

where $D(\Theta/T)$ represents the Debye integral, n is the number of atoms per formula unit. For an isotropic solid, Θ is expressed as

$$\Theta = \frac{\hbar}{K}[6\pi^2 V^{1/2} n]^{1/3} f(\sigma)\sqrt{\frac{B_S}{M}}. \tag{19}$$

where M is the molecular mass per formula unit, B_s the adiabatic bulk modulus, which can be approximated by the static compressibility

$$B_s \cong B(V) = V\left(\frac{d^2E(V)}{dV^2}\right). \tag{20}$$

The Poisson ratio σ is taken as 0.269. According to Refs. [32,34], $f(\sigma) = 0.822269$. For the Ta_4AlC_3, $n = 8$, $M = 786.8069915$ a.u. Therefore, the non-equilibrium Gibbs function $G^*(V; P, T)$ as a function of $(V; P, T)$ can be minimized with respect to volume V as follows:

$$\left(\frac{\partial G^*(V; P, T)}{\partial V}\right)_{P,T} = 0. \tag{21}$$

By solving Eq. (21), the isothermal bulk modulus and other thermal properties such as heat capacity at constant volume C_V, the heat capacity at constant pressure C_P, and thermal expansion α are respectively taken as:

$$B_T(P, T) = -V\left(\frac{\partial P}{\partial V}\right) = V\left(\frac{\partial^2 G^*(V; P, T)}{\partial V^2}\right)_{P,T}. \tag{22}$$

$$C_V = 3nk\left[4D\left(\frac{\Theta}{T}\right) - \frac{3\Theta/T}{e^{\Theta/T} - 1}\right], \tag{23}$$

$$\alpha = \frac{\gamma C_V}{B_T V}, \tag{24}$$

$$C_P = C_V(1 + \alpha\gamma T). \tag{25}$$

where γ represents the Grüneisen parameter and it is expressed as $\gamma = -(\mathrm{d}\ln\Theta(V)/\mathrm{d}\ln V)$.

3. Results and discussion

3.1. Elasticity

In Table 2, we present the pressure dependence of the elastic constants c_{ij} and the aggregate elastic modulus (B, G) of α-Ta_4AlC_3 at zero temperature and different pressures. It is found that the five elastic constants increase monotonically with the applied pressure. c_{11} and c_{33} increase quickly with the increasing pressure, and c_{13} has a moderate increase as well as c_{12} and c_{44}. It can be seen from Table 2 that $c_{33} < c_{11}$. The implication of this is that the atomic bonds along the {0 0 1} planes between nearest neighbors are weaker than those along the {1 0 0} plane. Moreover, the bulk moduli B are sensitive to pressure as compared with shear moduli G.

Table 2

The calculated elastic constants c_{ij} (GPa), and aggregate elastic moduli (B, G, E/GPa), the quotient of bulk to shear modulus (B/G), the Poisson's ratio (ν), the Debye temperature (Θ_D/K) of the α-Ta_4AlC_3 under pressure (GPa) at zero temperature.

	P						
	0	5	10	20	30	40	50
c_{11}	492.79	535.08	569.23	623.69	677.47	730.88	778.86
c_{12}	160.72	172.94	181.85	211.49	241.00	261.88	288.03
c_{13}	154.77	168.65	180.74	216.40	253.56	283.07	316.70
c_{33}	417.95	459.51	492.68	556.94	616.30	645.26	697.80
c_{44}	191.70	212.74	229.00	252.62	281.38	307.62	329.48
B	259.62	282.61	301.32	343.26	385.05	417.72	455.12
G	141.66	155.77	167.01	180.74	195.69	210.77	222.82
E	359.58	394.78	422.91	461.27	502.02	541.28	574.67
B/G	1.83	1.81	1.80	1.90	1.97	1.98	2.04
ν	0.269	0.267	0.266	0.276	0.283	0.284	0.290
Θ_D	336.30	351.48	362.85	375.99	389.76	402.90	412.97

As known, the elastic constants determine the response of the crystal to external forces. They play an important part in determining the strength of the material. The high (low) quotient of bulk to shear modulus (B/G) value is associated with ductility (brittleness) [30]. The critical value which separates ductile and brittle materials is about 1.75. It is interesting to try to understand the microscopic origin of this empirical parameter. The calculated values of the B/G (>1.75) decrease at first then increase with pressures which means that pressure can reduce or improve ductility.

The Young's modulus E and Poisson's ratio ν are important for technological and engineering applications. Young's modulus is defined as the ratio between stress and strain, and is used to provide a measure of the stiffness of the solid, i.e., the larger the value of E, the stiffer is the material. The Young's modulus and Poisson's ratio increase with applied pressure (Table 2).

The elastic anisotropy of a crystal has an important implication in engineering science since it is highly correlated with the possibility to induce microcracks in the materials [35]. So, the anisotropy factor was evaluated to provide insight on the elastic anisotropy of the α-Ta_4AlC_3. The percentages of elastic anisotropy under pressures for bulk modulus A_B and shear modulus A_G in polycrystalline materials are important, can be obtained by the equations as follows:

$$A_B = \frac{B_V - B_R}{B_V + B_R}, \qquad A_G = \frac{G_V - G_R}{G_V + G_R} \tag{26}$$

A value of zero represents elastic isotropy and a value of 100% is the largest possible anisotropy. The percentage of bulk and shear anisotropies are listed in Fig. 2. It shows that α-Ta_4AlC_3 is largely isotropic in bulk and slightly anisotropic in shear at pressures or not.

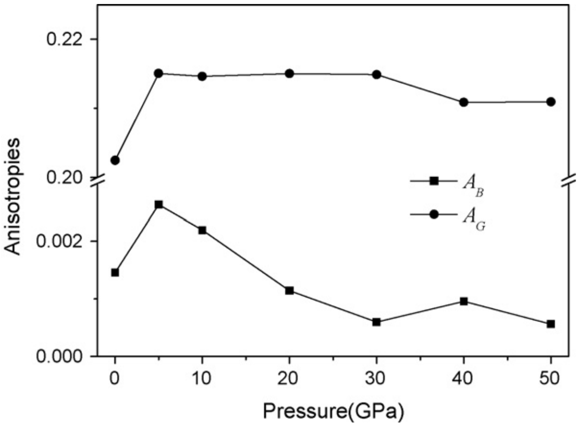

Fig. 2. The percentage of bulk and shear anisotropies of α-Ta_4AlC_3 as functions of pressure P.

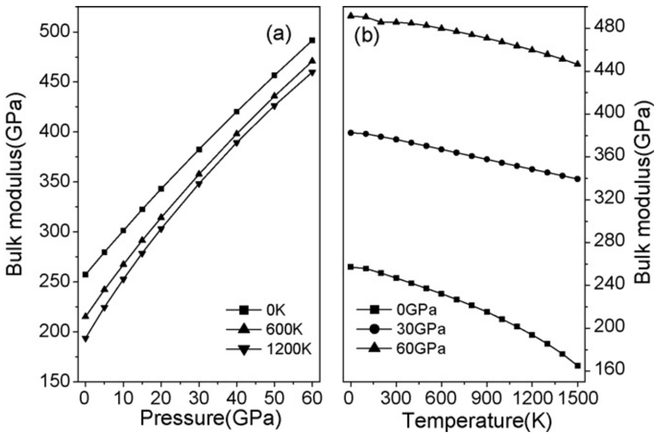

Fig. 3. Pressure (a) and temperature (b) dependence of the isothermal bulk modulus for α-Ta_4AlC_3.

3.2. Other thermal properties

Fig. 3 presents the relations of the isothermal bulk modulus as a function of temperature T up to 1500 K at P = 0, 30, and 60 GPa, respectively. When T < 200 K, the isothermal bulk modulus is nearly a constant, but it drops remarkably when T > 200 K, which is in accordance with the relationships between the ratio V/V_0 and pressure P as shown in Fig. 1. It demonstrates that dramatic volume variation leads to the rapid decreases in the isothermal bulk modulus. One can find that the effect of the temperature T on the isothermal bulk modulus is less important than that of the pressure P on it.

The calculated heat capacity at constant pressure C_P and heat capacity at constant volume C_V with the temperature T at different pressure P are shown in Fig. 4. The difference between C_P and C_V is very small at low temperatures. However, at high temperatures, the C_V approaches to the constant, C_P increases monotonously with the increment of the temperatures. The values follow the Debye model at low temperature ($C_V(T) \sim T^3$) and the classical behavior ($C_V(T) \sim 3R$ for mono-atomic solids) is found at sufficient high temperatures, obeying Dulong and Petit's rule. From Fig. 4, one can also see that the heat capacity increases with the temperatures at the same pressure and decreases with the pressures at the same temperature, the influences of the temperature on the heat capacity are much more significant than that of the pressure on it.

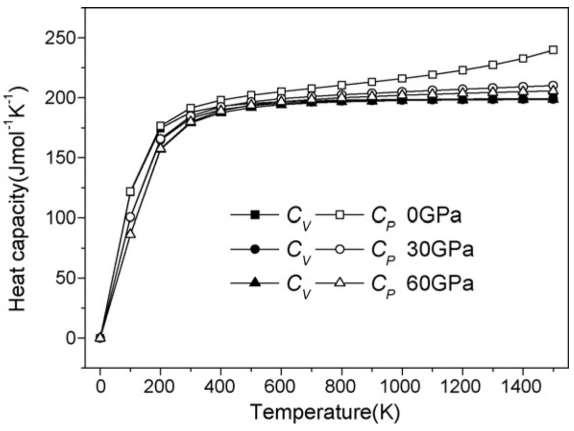

Fig. 4. Temperature dependence of the heat capacity for α-Ta_4AlC_3.

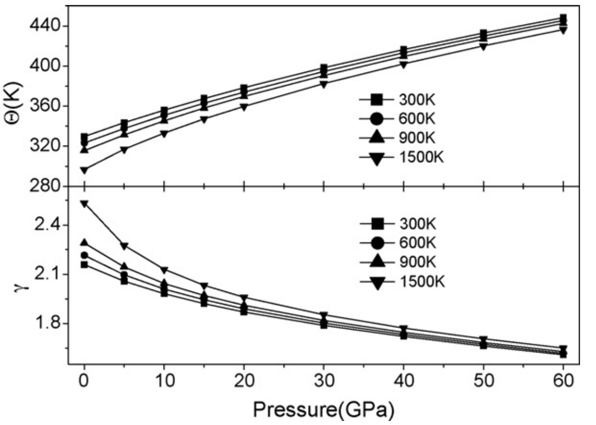

Fig. 5. Variation of the Debye temperature Θ and Grüneisen parameter γ with pressure.

The Debye temperature is a fundamental parameter of a material which is linked to many physical properties such as specific heat, elastic constants, and melting point [36]. The Debye temperature and the Grüneisen parameter at various temperatures and different pressures are presented in Fig. 5. Our calculated Debye temperature at $T = 0\,\mathrm{K}$ is $333.75\,\mathrm{J\,mol^{-1}\,K^{-1}}$, which is in agreement with the result ($336.3\,\mathrm{J\,mol^{-1}\,K^{-1}}$) from Eq. (13). From Fig. 5, one can find: (a) when the temperature keeps constant, the Debye temperature increases almost linearly with applied pressures, while the Grüneisen parameter decreases smoothly with pressures. (b) When the pressure keeps constant, the Debye temperature decreases with the increasing temperatures, while the Grüneisen parameter increases with the increasing temperatures, in virtue of the fact that the effect of increasing pressure on the material is the same as decreasing temperature of the material. (c) The Debye temperature at the temperature of 1500 K is lower than that at 300 K, which shows the fact that the vibration frequency of the particles in α-$\mathrm{Ta_4AlC_3}$ changes with the pressures and the temperatures.

The thermal expansion coefficient α with temperature and pressure for α-$\mathrm{Ta_4AlC_3}$ is presented in Fig. 6. From Fig. 6(a), the thermal expansion coefficient α increases with T^3 at low temperatures, gradually approaches a linear increase at high temperatures, and then the increasing trend becomes gentler. The effects of pressure on the thermal expansion coefficient α are very small at low temperatures; the effects are increasingly obvious as the temperature increases. As pressure increases, the thermal expansion coefficient α decreases rapidly and the effects of temperature become less and less pronounced, resulting in linear high-temperature behavior. It is noteworthy that the high-temperature dependence of the thermal expansion coefficient α is not linear at low pressures (0 and 5 GPa); this is an indication of the inadequacy of the quasi-harmonic approximation at high temperatures and low pressures. It can be found that the thermal expansion coefficient α converges to a constant value at high temperatures and pressures. However, from Fig. 6(b), as the pressure increases, the thermal expansion coefficient α decreases almost exponentially, and the higher the temperature is, the faster the thermal expansion coefficient α decreases. This shows that the effect of temperature is much greater than that of pressure on the thermal expansion coefficient α.

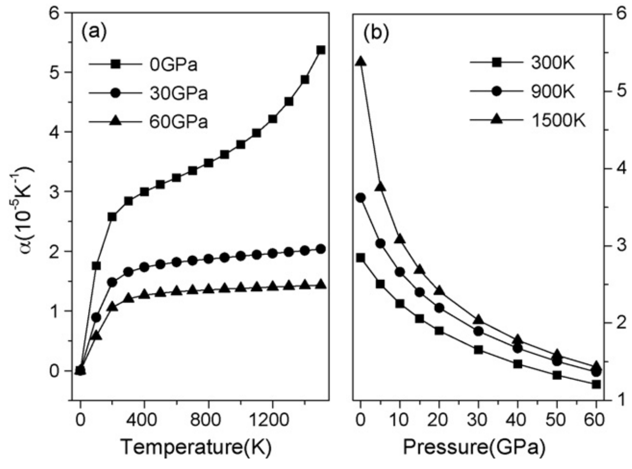

Fig. 6. Temperature (a) and pressure (b) dependence of the thermal expansion coefficient α for α-$\mathrm{Ta_4AlC_3}$.

4. Conclusions

The structural properties and elastic constants of α-$\mathrm{Ta_4AlC_3}$ at high pressure are computed by the ultrasoft pseudopotentials within the generalized gradient approximation in the frame of density functional theory. We carry out total energy calculations over a wide range of volumes from $0.8V_0$ to $1.2V_0$, and obtain the equilibrium ratio of the normalized volume V/V_0 for a given volume. The obtained pressure dependence of the normalized volume is in excellent agreement with the experimental result.

The elastic constants, the aggregate elastic modulus (B, G, E), Poisson's ratio, and the anisotropy of α-$\mathrm{Ta_4AlC_3}$ at high pressure in the range of 0–50 GPa are also calculated. The elastic constants indicate that the atomic bonds along the {0 0 1} planes between nearest neighbors are weaker than those along the {1 0 0} plane. The calculated values of the B/G (>1.75) decrease at first then increase with pressures which means that pressure can reduce or improve ductility. The calculated percentages of elastic anisotropy A_B and A_G show that α-$\mathrm{Ta_4AlC_3}$ is largely isotropic in bulk and slightly anisotropic in shear.

The other thermodynamic properties are predicted using the quasi-harmonic Debye model. It is found that the high temperature leads to a smaller adiabatic bulk modulus, a smaller Debye temperature, a larger Grüneisen parameter, a larger heat capacity, and a larger thermal expansion coefficient at constant pressure. But the high pressure gives birth to a lager isothermal bulk modulus, a larger Debye temperature, a smaller Grüneisen parameter, a smaller heat capacity, and a smaller thermal expansion coefficient at constant temperature. The thermal expansion coefficient and heat capacity at constant volume are shown to converge to a nearly constant value at high pressures and temperatures.

Acknowledgements

This project was supported by the National Natural Science Foundation of China under Grant No. 40804034, and by the Luoyang Normal University Science Foundation for Youths under Grant No. 2008-NQJJ-014.

References

[1] N.A. Phatak, S.K. Saxena, Y. Fei, J. Hu, J. Alloys Compd. 474 (2009) 147.
[2] N.A. Phatak, S.R. Kulkarni, V. Drozd, S.K. Saxena, L. Deng, Y. Fei, J. Hu, W. Luo, R.A.I. Salama, T. El-Raghy, M.W. Barsoum, J. Alloys Compd. 463 (2008) 220.
[3] C.L. Yeh, Y.G. Shen, Prog. J. Alloys Compd. 470 (2009) 424.
[4] X. He, Y. Bai, Y. Li, C. Zhu, M. Li, Solid State Commun. 149 (2009) 564.
[5] C.F. Hu, J. Zhang, J.M. Wang, F.Z. Li, J.Y. Wang, Y.C. Zhou, J. Am. Ceram. Soc. 91 (2008) 636.
[6] J.P. Palmquist, T. El-Raghy, J. Höwing, O. Wilhelmsson, M. Sundberg, 30th International Conference on Advanced Ceramics and Composites, 2006, (Abstract #ICACC-S1-184-2006).
[7] B. Manoun, S.K. Saxena, T. El-Raghy, M.W. Barsoum, Appl. Phys. Lett. 88 (2006) 201902.
[8] Z.J. Lin, M.J. Zhuo, Y.C. Zhou, M.S. Li, J.Y. Wang, J. Mater. Res. 21 (2006) 2587.

[9] Z.J. Lin, M.J. Zhuo, Y.C. Zhou, M.S. Li, J.Y. Wang, J. Am. Ceram. Soc. 89 (2006) 3765.

[10] P. Eklund, J.P. Palmquist, J. Höwing, D.H. Trinh, T. El-Raghy, H. Högberg, L. Hultman, Acta Mater. 55 (2007) 4723.

[11] J. Etzkorn, M. Ade, H. Hillebrecht, Inorg. Chem. 46 (2007) 1410.

[12] J. Wang, J. Wang, Y. Zhou, Z. Lina, C. Hu, Scripta Mater. 58 (2008) 1043.

[13] Y.L. Du, Z.M. Sun, H. Hashimoto, W.B. Tian, Solid State Commun. 145 (2008) 461.

[14] Y.L. Du, Z.M. Sun, H. Hashimoto, W.B. Tian, Solid State Commun. 147 (2008) 246.

[15] X.H. Deng, B.B. Fan, W. Lu, Solid State Commun. (2009), doi:10.1016/j.ssc.2008.12.041.

[16] W. Lu, X.H. Deng, H. Wang, H.T. Huang, L.L. He, J. Mater. Res. 23 (2008) 2350.

[17] L. Louail, D. Maouche, A. Roumili, F. Ali Sahraoui, Mater. Lett. 58 (2004) 2975.

[18] P. Hohenberg, W. Kohn, Phys. Rev. B 136 (1964) 384.

[19] D. Vanderbilt, Phys. Rev. B 41 (1990) 7892.

[20] Z. Wu, R.E. Cohen, Phys. Rev. B 73 (2006) 235116.

[21] M.D. Segall, P.J.D. Lindan, M.J. Probert, C.J. Pickard, P.J. Hasnip, S.J. Clark, M.C. Payne, J. Phys.: Condens. Matter 14 (2002) 2717.

[22] F. Birch, Phys. Rev. 71 (1947) 809.

[23] J. Wang, S. Yip, S.R. Phillpot, D. Wolf, Phys. Rev. B 52 (1995) 12627.

[24] D.C. Wallace, Thermodynamics of Crystals, Wiley Publication, New York, 1972, pp. 20–22.

[25] B.B. Karki, G.J. Ackland, J. Crain, J. Phys.: Condens. Matter 9 (1997) 8579.

[26] T.H.K. Barron, M.L. Klein, Proc. Phys. Soc. 85 (1965) 523.

[27] K. Tsubouchi, N. Mikoshiba, IEEE Trans. Sonics Ultrason. Su-32 (1985) 634.

[28] A. Reuss, Z. Angew. Math. Mech. 9 (1929) 49.

[29] G.V. Sin'ko, N.A. Smirnow, J. Phys.: Condens. Matter 14 (2002) 6989.

[30] O.L. Anderson, J. Phys. Chem. Solids 24 (1963) 909.

[31] M.A. Blanco, E. Francisco, V. Luana, Comput. Phys. Commun. 158 (2004) 57.

[32] M.A. Blanco, A.M. Pendás, E. Francisco, J.M. Recio, R. Franco, J. Mol. Struct. (Theochem.) 368 (1996) 245.

[33] M. Flórez, J.M. Recio, E. Francisco, M.A. Blanco, A.M. Pendás, Phys. Rev. B 66 (2002) 144112.

[34] E. Francisco, J.M. Recio, M.A. Blanco, A.M. Pendás, J. Phys. Chem. 102 (1998) 1595.

[35] M. Born, K. Huang, Dynamical Theory of Crystal Lattices, Clarendon, Oxford, 1954.

[36] P. Ravindran, L. Fast, P.A. Korzhavyi, B. Johnnsson, J. Wills, O. Eriksson, J. Appl. Phys. 84 (1998) 4891.